

RSC Advances



This is an *Accepted Manuscript*, which has been through the Royal Society of Chemistry peer review process and has been accepted for publication.

Accepted Manuscripts are published online shortly after acceptance, before technical editing, formatting and proof reading. Using this free service, authors can make their results available to the community, in citable form, before we publish the edited article. This *Accepted Manuscript* will be replaced by the edited, formatted and paginated article as soon as this is available.

You can find more information about *Accepted Manuscripts* in the [Information for Authors](#).

Please note that technical editing may introduce minor changes to the text and/or graphics, which may alter content. The journal's standard [Terms & Conditions](#) and the [Ethical guidelines](#) still apply. In no event shall the Royal Society of Chemistry be held responsible for any errors or omissions in this *Accepted Manuscript* or any consequences arising from the use of any information it contains.

ARTICLE

Functionalizable Red Emitting Calcium Sensor Bearing a 1,4-triazole Chelating Moiety

Cite this: DOI: 10.1039/x0xx00000x

Mayeul Collot,^{*a} Christian Wilms,^b Jean-Maurice Mallet^{c, d, e}Received 00th January 2012,
Accepted 00th January 2012

DOI: 10.1039/x0xx00000x

www.rsc.org/

Herein we developed a functionalizable OFF-ON red emitting fluorescent calcium probe based on a new chelating system formed by CuAAC click chemistry (Huisgen cycloaddition). The pro-sensor **7** which is not sensitive to Ca²⁺, contains an alkyne moiety that, upon click reaction, forms a chelating group involving the 1,4-triazole. Probe **10** exhibited a good sensitivity towards calcium (K_d= 5.8 μM) and zinc (5.6 μM) with a high dynamic range (65 fold fluorescence increase), high quantum yield (0.59) and showed very low fluorescence enhancement in presence of high concentration of Mg²⁺. We extended this method and generated two dextran conjugates in order to compare their sensing properties with those of the molecular form **10**.

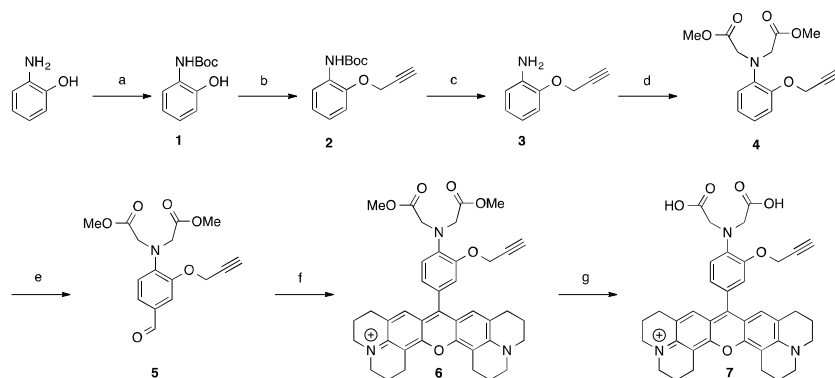
1 Introduction

Ca²⁺ is an ubiquitous second messenger involved in numerous intracellular signalling cascades. Therefore fluorescent Ca²⁺ indicators are indispensable tools for studying spatiotemporal fluctuations of intracellular free Ca²⁺ concentration ([Ca²⁺]_i).^{1,2} The first fluorescent Ca²⁺ probes were introduced by Tsien and colleagues in the mid-eighties involving the BAPTA (1,2-bis(o-aminophenoxy)ethane-*N,N,N',N'*-tetraacetic acid) chelating moiety.³ Consequently, most Ca²⁺ indicators, and certainly those that work best, combined BAPTA with fluorescein derivatives and hence emit yellow/green fluorescence.^{4,5} However, the increasing use of cells transfected with fluorescent proteins (FPs), of FP expressing transgenic mice for targeting identified subpopulations of cells, together with the advent of optical techniques for purposes other than imaging require the development of new red Ca²⁺ probes.^{6,7} We recently reviewed the red-fluorescent calcium indicators allowing photoactivation and multi-color imaging⁸ and contributed in this field by developing a new family of functionalizable red emitting calcium sensors based on BAPTA, the Ca-Rubies, with various dissociation constants (K_d).⁹ Cellular Ca²⁺ signals cover concentrations from near 100 nM for the basal free [Ca²⁺]_i of most mammalian cells to >100 μM at the peak of Ca²⁺ microdomains. A Ca²⁺ probe works best if its dissociation constant is close to the intracellular Ca²⁺ concentration. However, if the K_d is too large, Ca²⁺ measurement will be insensitive; on the other hand, if the calcium concentration is higher or is involved in fast transients, the probe with small K_d could saturate quickly and results in inaccurate measurement. Therefore, it is of great importance to develop fluorescent sensors with micromolar range K_d for the measurement of accurate intracellular Ca²⁺ fast transients. To our knowledge, only few alternatives to BAPTA systems have been reported as new calcium sensors. APTRA (aminophenol triacetic acid) developed by Levy et al.¹⁰ has a poor selectivity for Ca²⁺ over other divalent ions. Other systems like MOBHA (2-(2'-morpholino-2'-oxoethoxy)-*N,N*-bis(hydroxycarbonyl methyl)aniline)¹¹ or sensors based on PEGylated moieties either display low affinities or aggregate under biological conditions.¹² Most of fluorescent metal sensors tend to compartmentalize in cells due to their hydrophobicity, therefore the capability of functionalization can lead to much higher hydrophilicity or specificity and thus extend the scope as the probe can be linked for instance to polymer, particles, peptide or dextran.

In this work, we describe an unprecedented system where the pro-sensor **7** becomes a calcium sensor upon functionalisation via Huisgen cycloaddition by completing the coordination sphere of calcium involving the N-3 of the newly formed 1,4-triazole moiety (Abstract scheme). These sensors (molecular form and dextran conjugates) based on the PET (Photoinduced Electron Transfer) quenching phenomena display a bright red fluorescence upon binding to Ca²⁺ with low micromolar range K_ds combined to a strong fluorescence enhancement and a very low sensitivity towards Mg²⁺.

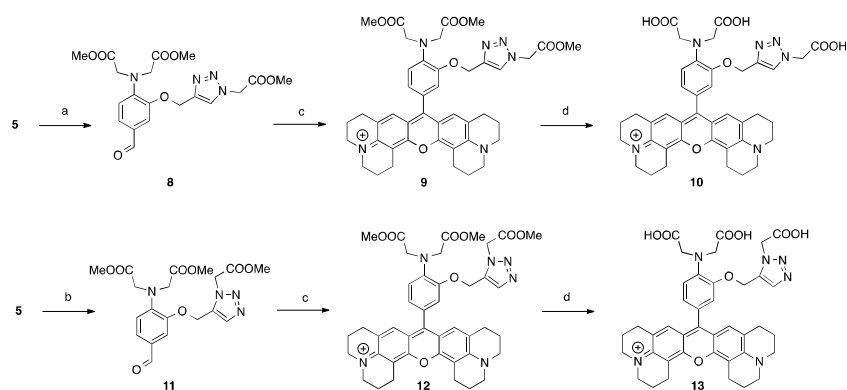
2 Results and Discussion

Huisgen 1,3-dipolar azide–alkyne cycloaddition has become the most popular “click chemistry” type reaction due to its efficiency and the availability of the reactants.¹³ 1,4-triazole moieties formed after this ligation have already successfully been used to form complexes with metals^{14,15} and also served for the development of fluorogenic sensors.^{16,17,18,19} To this regard, **7** was designed to provide a functionalisable fluorophore with a new chelating pattern involving the *N,N*-diacetic acid aminophenoxy moiety taken from BAPTA as well as the nitrogen-3 of the newly formed 1,4-triazole moiety making this system a “2 in 1” approach”. The synthesis starts with 2-aminophenol to obtain aldehyde **5** in 5 steps with an overall yield of 43%. **5** was then converted into the corresponding X-rhodamine **6** to give, after saponification, the clickable pro-sensor **7** (scheme 1).



Scheme 1. Synthesis of pro-sensor **7**. a) Boc₂O, MeOH, 80%; b) propargyl bromide; K₂CO₃, DMF, 80°C, 86%; c) TFA; d) Methyl bromoacetate, DIEA, ACN, 90°C, 94% over 2 steps; e) POCl₃, DMF, 80°C, 67%; f) 8-hydroxyjulolidine, PTSA, propionic acid, then chloranil, 13%; g) KOH, MeOH, 76%.

5 was then involved in a Huisgen cycloaddition catalysed by Cu^I in order to afford the 1,4-triazole compound **8**, the latter was converted into the X-rhodamine **9** and finally saponified to yield the probe **10** (Scheme 2). In order to study the involvement of the N-3 of the triazole moiety, a 1,5-triazole isomer **13** of the sensor **10** was synthesised. **5** was reacted with methyl 2-azidoacetate in presence of a small amount (0.04 equivalent) of [RuClCp*(PPh₃)₂] as a catalyst²⁰ to furnish **11** which was transformed in two steps in **13** (Scheme 2). Isomers **10** and **13** only differ from the availability of a nitrogen atom of the triazole groups. Whereas **10** is able to form a chelate with the N-3 of its 1,4-triazole, the steric conformation of **13** does not allow the participation of any nitrogen atom to complete the chelation ability of the molecule.



Scheme 2. a) Methyl azidoacetate, CuSO₄·5H₂O, sodium ascorbate, Dioxane, Water, 83%; b) Methyl azidoacetate, [RuClCp*(PPh₃)₂], dioxane, 90°C, 90%; c) 8-hydroxyjulolidine, PTSA, propionic acid, then chloranil, 20% for **9**, 16% for **12**; d) KOH, MeOH, 81% for **10**, 76% for **13**.

The chelating properties of fluorescent sensors **7**, **10** and **13** were then investigated by fluorescence spectroscopy. First, the fluorescence enhancement ($\Delta F/F_0$) of the sensors in the presence of 3 equivalents of various metals (Ca²⁺, Cd²⁺, Cu²⁺, Fe³⁺, Hg²⁺, Mg²⁺, Mn²⁺ and Zn²⁺) was evaluated (Figure 1).

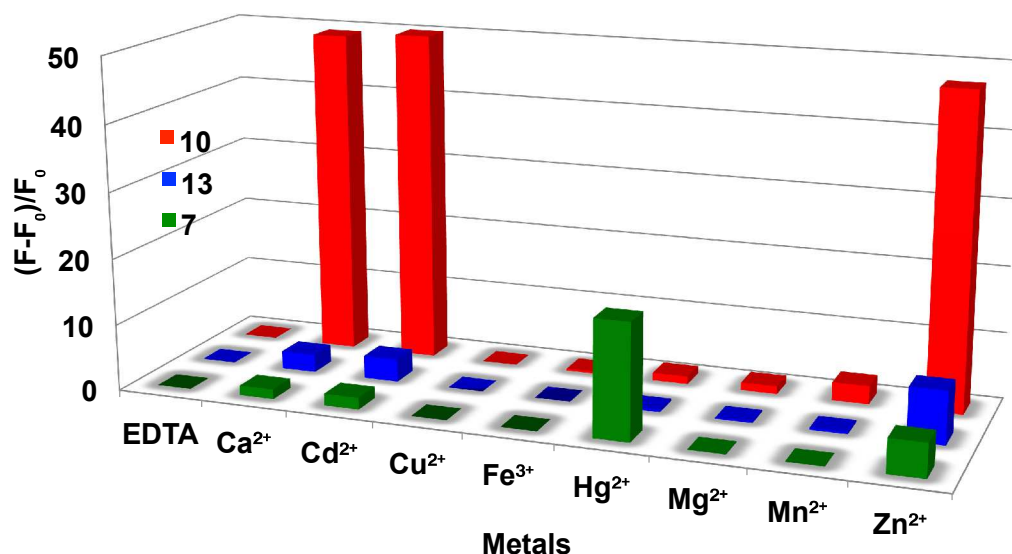
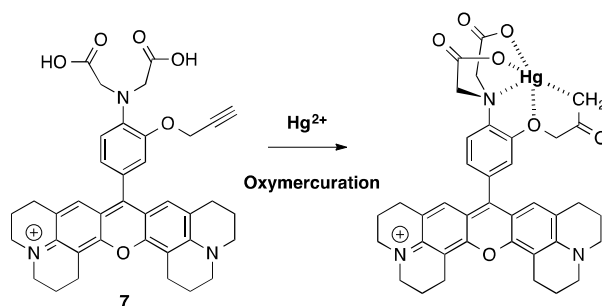


Figure 1. Fluorescence enhancement ($(F-F_0)/F_0$, with F_0 = Fluorescence Intensity in presence of EDTA 1 mM) of **7**, **13** and **10** (5 μ M, MOPS 30 mM, KCl 100 mM, pH 7.2) in presence of 3 equivalents (15 μ M) of various metals.

In the case of the pro-sensor **7**, the majority of tested metals did not trigger the fluorescence or only small enhancements were observed (Zn, 5 fold). Interestingly, **7** displayed a quite significant fluorescence enhancement in presence of Hg^{2+} with a $\Delta F/F_0$ of 17 fold. This could be explained by an oxymercuration^{21,22} reaction of the alkyne moiety of **7** leading to a stabilised organomercury complex (scheme 3).



Scheme 3. Proposed formation of stabilised mercury chelate via an oxymercuration reaction involving **7**.

Whereas **10** exhibits strong responses with Ca^{2+} , Cd^{2+} and Zn^{2+} up to 52 folds for Cd^{2+} and 49 for Ca^{2+} , **13** gave only weak fluorescence enhancements with Ca^{2+} and Cd^{2+} and a $\Delta F/F_0$ of 7.9 fold with Zn^{2+} (Figure 1). These results suggest that the N-3 of the 1,4-triazole is involved in the stabilisation of a calcium complex. This hypothesis was confirmed by the dissociation constants measurements. **10** exhibited substantially the same high affinity for Ca^{2+} and Zn^{2+} ($K_d \text{Ca}^{2+} = 5.84 \pm 0.21 \mu\text{M}$, $K_d \text{Zn}^{2+} = 5.68 \pm 0.14$) whereas **7** and **13** have low affinity towards these metals (table 1). Job's plot evidenced that **10** formed a 1:1 complex with Ca^{2+} which displays a bright red fluorescence at 604 nm with an increase of quantum yield of 78 fold and a fluorescence enhancement of 65 fold (Figure 2). In view to these results, **10**, which has a $K_{d\text{Ca}}$ close our previously published CaRuby-F, can be considered as an efficient Ca^{2+} sensor as the concentration of Zn^{2+} in cells is nanomolar, far below its $K_{d\text{Zn}}$.²³

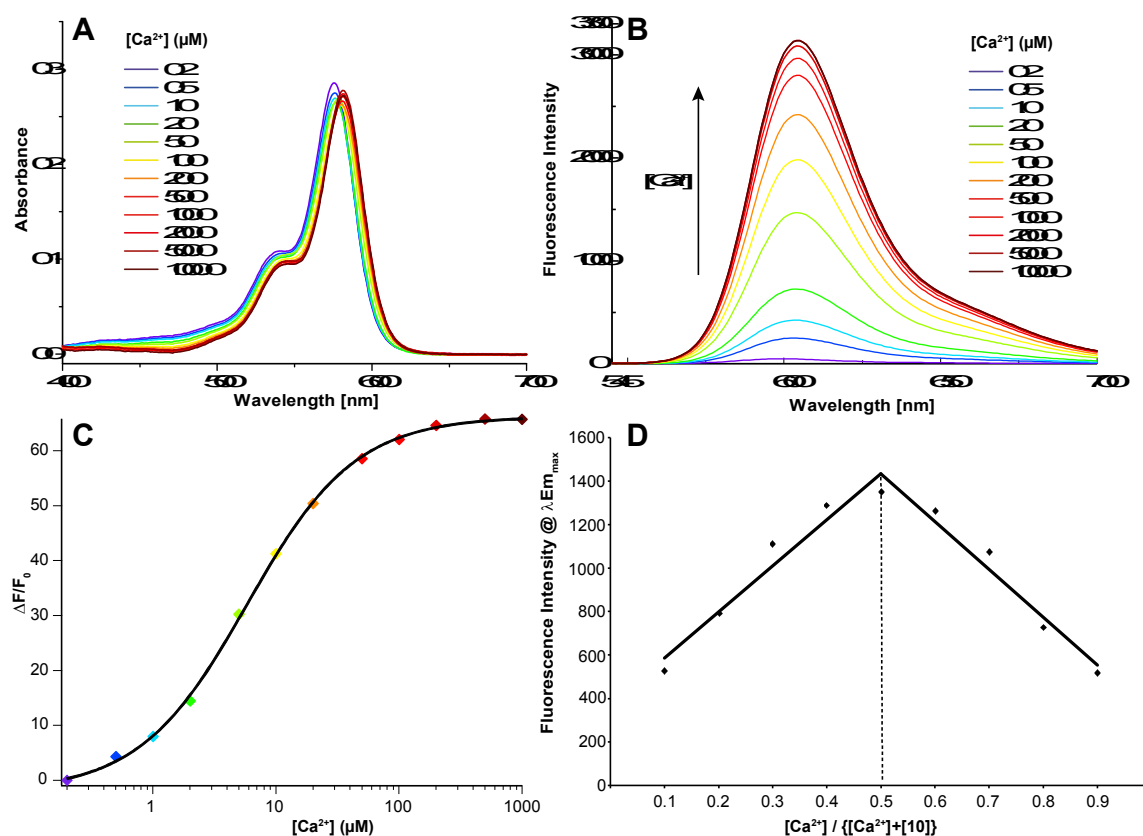


Figure 2. (A) UV-Visible absorption spectra and (B) emission spectra ($\lambda_{\text{ex}} = 535 \text{ nm}$) of **10** ($5 \mu\text{M}$, MOPS 30 mM , KCl 100 mM) at increasing concentration of Ca^{2+} . (C) Plot of fluorescence enhancement ($(F-F_0)/F_0$, with F_0 = Fluorescence Intensity in presence of EDTA 1 mM) of **10** ($5 \mu\text{M}$, MOPS 30 mM , KCl 100 mM , pH 7.2) vs. increasing concentration of Ca^{2+} . The fit line, according to Hill's equation, yielded the K_d . (D) Job's plot of **10** ($[\text{Ca}^{2+}], [\text{10}] = 5 \mu\text{M}$) determined a Ca^{2+} complex with a 1:1 stoichiometry.

Compound	λ_{Abs}^a (nm)	ϵ (M^{-1} cm^{-1})	λ_{Em}^a (nm)	Φ_{EGTA}^b	Φ_{Ca}	$\Phi_{\text{Ca}}/\Phi_{\text{EGTA}}$	$K_{d_{\text{Zn}}}(\mu\text{M})^c$	$K_{d_{\text{Ca}}}(\mu\text{M})^c$
7	577-582	48,000	606-608	0.004	0.06	6	205 ± 40	N/A ^d
10	576-581	54,000	599-604	0.007	0.59	78	5.6 ± 0.1	5.8 ± 0.2
13	576-580	80,000	601-605	0.005	0.29	54	118.91 ± 3.9	448 ± 10

^a Calcium free [EGTA] = 1 mM and $[\text{Ca}^{2+}] = 1 \text{ mM}$

^b Calcium free [EGTA] = 1 mM

^c Obtained by fitting the data with Hill's equation

^d Fitting the data with Hill's equation provided no result

Table 1. Physicochemical properties of the sensors ($5 \mu\text{M}$, MOPS 30 mM , KCl 100 mM , pH 7.2)

A fluorescent calcium probe intended for use in cellular assays should fulfil several criteria. First the sensitivity to pH variations met in cells should not interfere with the signal obtained in response to Ca^{2+} . pH sensitivity of **10** was evaluated and whereas the pKa value was found to be in the physiological range (5.93 ± 0.07), the fluorescence enhancement from pH 7.5 to pH 4.5 is only 1.9 fold (Figure S2) which is negligible in regard of the much higher fluorescence increase (65 fold) provoked by Ca^{2+} . A major drawback in molecular Ca^{2+} probes is that their hydrophobicity often leads to compartmentalization in organelles such as plasma membrane, ER (Endoplasmic Reticulum), mitochondria, etc. To avoid this issue, probes can be linked to non toxic and inert dextrans which are effective water-soluble carriers for dyes and indicators.²⁴ Dextran conjugates have enhanced hydrophilicity and hence, facilitate the distribution of the probe in the cytosol through microinjection.²⁵ Therefore, pro-sensor **7** was linked via click chemistry to two prepared azido-dextran (obtained from dextran of $1,500 \text{ MW}$ and dextran 6000 MW , see SI) (figure 3A) in order to study the influence of the dextran carrier on the Ca^{2+} sensing properties. Despite dextran conjugates $1,500$ and $6,000$ displayed slightly higher $K_{d_{\text{Ca}}}$ of $16.3 \pm 0.6 \mu\text{M}$ and $18.3 \pm 0.8 \mu\text{M}$ respectively (figure 3B), their

fluorescence enhancement, respectively 41 and 36 fold, make them efficient calcium sensors. The slight drop of sensitivity (fluorescence enhancement) could be attributed to the formation of dark H-aggregates due to the proximity of the sensors within the dextran polymer as the absorbance spectra exhibited a second band at 545 nm (figure 3C). This phenomenon could be reduced by decreasing the number of sensors per dextran molecules (14 sensors per 100 glucose units). The shift of the $K_{d_{Ca}}$ values could be attributed to an effect that we recently described as a remote control.²⁶ Even though the coordination sphere is not affected by what the probe is linked to, the close environment of the complex can influence the dissociation constant. While, in the case of **10**, a close negative charge (COO^-) seems to increase the affinity of the sensor towards Ca^{2+} , a side PEG chain, in the case of the dextran conjugates, slightly lower this affinity, these results are in accordance to what we already observed.

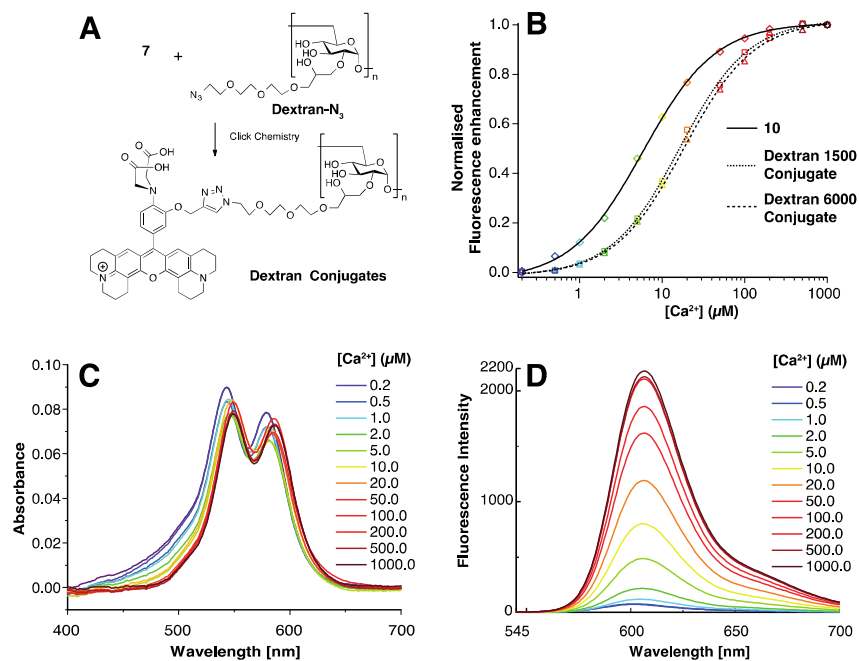


Figure 3. (A) Synthesis of Dextran conjugates by Click Chemistry ($CuSO_4 \cdot 5H_2O$, sodium ascorbate, DMF, water, 76% for dextran 1500, 80% for dextran 6000). (B) Normalized fluorescence enhancement ($(F-F_0)/F_0$, with F_0 = Fluorescence Intensity in presence of EDTA 1 mM) of **10** and its dextran conjugates (MOPS 30 mM, KCl 100 mM, pH 7.2) vs. increasing concentration of Ca^{2+} . The fit lines, according to Hill's equation, yielded the K_{ds} . (C) Absorbance spectra and (D) emission spectra (λ_{Ex} = 535 nm) of Dextran 6000 conjugate (MOPS 30 mM, KCl 100 mM) at increasing concentration of Ca^{2+} .

Finally, since Mg^{2+} is buffered in the cytoplasm at concentration in the sub-millimolar range, it is of extreme importance that the sensor remains insensitive to Mg^{2+} at high concentrations to avoid background fluorescence. Figure 4 shows that **10** and its dextran conjugates were virtually non sensitive to high concentration of Mg^{2+} (1 mM), moreover the presence of an equimolar concentration of Mg^{2+} and Ca^{2+} does not influence the fluorescence enhancement of the sensors.

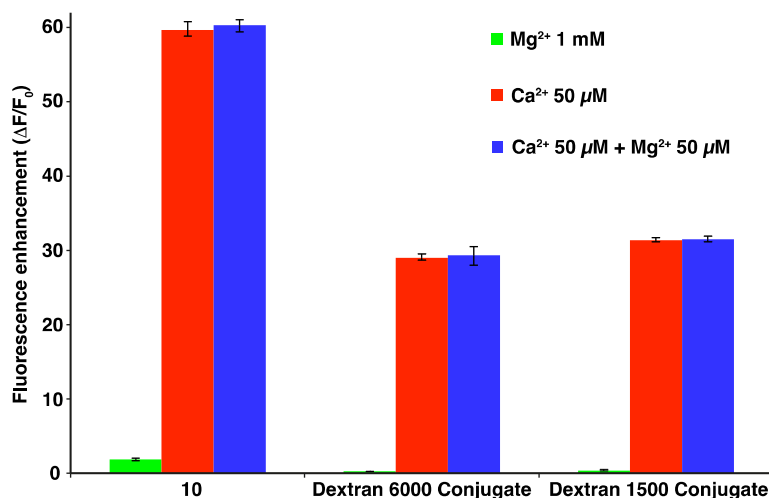


Figure 4. Fluorescence enhancement ($(F-F_0)/F_0$, with F_0 = Fluorescence Intensity in presence of EDTA 1 mM) of **7** and its dextran conjugates (MOPS 30 mM, KCl 100 mM, pH 7.2) in presence of Mg^{2+} (1 mM), Ca^{2+} (50 μ M) and a mixture of Ca^{2+} and Mg^{2+} (50 μ M).

The properties of these dextran conjugates are attractive for potential cell biology applications. In the case of measurement of intracellular calcium ion ($[Ca^{2+}]_i$) transients in myocytes, it was shown that low affinity indicators, like Fura-2 ($K_{d_{Ca}} \sim 240$ nM), yielded greater peak amplitude of stimulated $[Ca^{2+}]_i$ transients than those obtained with high affinity indicators (Fura-2 $K_{d_{Ca}} = 240$ nM). This is partially due to the detrimental buffering effect of high affinity indicators.²⁷ Therefore, the dextran conjugates we present, could offer an interesting alternative to Fura-2 with no sensitivity towards Mg^{2+} , an enhanced brightness, red-shifted absorption and emission spectra, lower K_d s and a better hydrophilicity brought by the dextran molecules.

3 Conclusion

We developed a new Ca^{2+} sensor system where the newly formed 1,4-triazole moiety is involved in the chelation pattern. The pro-sensor **7** is insensitive to Ca^{2+} and thus can be used to functionalise any azide decorated (bio)molecule, polymers or chips without need to separating the precursor from the product. This system is readily accessible and represents a good alternative to micromolar range BAPTA based sensors. Moreover, its sensitivity and brightness combined to its functionalisable capability makes this system a valuable tool for potential monitoring of Ca^{2+} transients. These new indicators (molecular sensor **10** and dextran conjugates) feature very good properties and we believe that as red, Mg^{2+} insensitive, low affinity fluorescent Ca^{2+} probes, they will strengthen the arsenal of fluorescent Ca^{2+} sensors.

4 Experimental

4.1 Materials and general methods

All the solvents were of analytical grade. Chemicals were purchased from commercial sources. The salts used in stock solutions of metal ions were $CaCl_2 \cdot 2H_2O$, $CdCl_2$, $CuCl_2 \cdot 2H_2O$, $FeCl_3 \cdot 6H_2O$, $HgCl_2$, KCl, $MgCl_2 \cdot 6H_2O$, $MnCl_2 \cdot 4H_2O$, NaCl, $Zn(NO_3)_2$. 1H -NMR and ^{13}C -NMR were measured on a Bruker Avance III-300 MHz spectrometer with chemical shifts reported in ppm (TMS as internal standard). Mass spectra were measured on a Focus GC / DSQ II spectrometer (ThermoScientific) for IC and an API 3000 spectrometer (Applied Biosystems, PE Sciex) for ES. All pH measurements were made with a Mettler Toledo pH-Meter. Fluorescence spectra were recorded on a JASCO FP-8300 spectrofluorometer. Absorption spectra were measured on a VARIAN CARY 300 Bio UV-Visible spectrophotometer. All measurements were done at a set temperature of 25°C. The purity of the dyes was checked by RP-HPLC C-18, eluant: ACN 0.1% TFA/Water 0.1% TFA, method: 20/80 to 100/0 within 20 min then 100/0 for 10 min. detection at $\lambda_{Abs} = 254$ nm.

4.2 Synthesis

1 was synthesized according to a published protocol.²⁸

2. To a solution of **1** (3.200 g, 15.31 mmol) in DMF (30 mL) were added propargyl bromide 80 wt. % in toluene (2.52 mL, 22.96 mmol, 1.5 eq) and K_2CO_3 (3.168 g, 22.96 mmol, 1.5 eq). The solution was heated at 80°C for 5h before being cooled down to room temperature. The

solvents were evaporated and the product was extracted with EtOAc washed with water (3 times) and brine (2 times). The organic phase was dried over MgSO₄, filtered and evaporated. The crude was purified by column chromatography on silica gel (Cyclohexane/EtOAc : 9/1) to obtain 3.28 g of **2** (86%) as a yellowish syrup. Rf=0.69 (Cyclohexane/EtOAc, 8/2). ¹H-NMR (300 MHz, CDCl₃): δ 8.13 (d, *J* = 5.3 Hz, 1H, HAr), 7.10 (s, 1H, NH), 7.02-7.00 (m, 3H, H Ar), 4.78 (d, *J* = 2.4 Hz, 2H, CH₂), 2.58 (t, *J* = 2.4 Hz, 1H, CH), 1.56 (s, 9H, tBu). ¹³C-NMR (75 MHz, CDCl₃): δ 152.72 (CO Boc), 145.54 (Cq Ar), 128.64 (Cq Ar), 122.21 (CH Ar), 122.15 (CH Ar), 118.53 (CH Ar), 111.74 (CH Ar), 80.42 (Cq tBu), 78.20 (C≡CH), 76.07 (C=C₂H), 56.47 (CH₂), 28.40 (tBu). MS (CI), calcd for C₁₄H₁₇NO₃ [M]⁺ 247.1, found 247.1, HRMS (CI), C₁₄H₁₇NO₃ [M]⁺ 247.1208, found 247.1195.

4. To a cooled (0°C) solution of **2** (3.280 g, 13.28 mmol) in DCM (20 mL) was added TFA (5 mL). The solution was allowed to stir at room temperature overnight. TFA was neutralized by addition of a saturated solution of NaHCO₃ to reach a pH of 8. The product was extracted with DCM and the solution was dried over MgSO₄, filtered and evaporated to obtain **3**. Rf=0.35 (Cyclohexane/EtOAc, 8/2). To a solution of **3** (1.923 g, 13.06 mmol) in acetonitrile (26 mL) were added methyl bromoacetate (3.69 mL, 39.84 mmol, 3 eq) and DIEA (6.92 mL, 39.84 mmol, 3 eq) before being warmed up to 90°C overnight. 2 more equivalent of both methyl bromoacetate and DIEA were then added to complete the reaction. The solution was stirred at 90°C over 6h. The solvents were evaporated, the product was extracted with DCM and washed with water. The organic phase was dried over MgSO₄, filtered and evaporated. The crude was purified by column chromatography on silica gel (Cyclohexane/EtOAc : 9/1) to obtain 3.64 g of **4** (94%) as a yellowish syrup. Rf=0.28 (Cyclohexane/EtOAc, 8/2). ¹H-NMR (300 MHz, CDCl₃): δ 6.95 (m, 4H, H Ar), 4.72 (d, *J* = 2.4 Hz, 2H, OCH₂), 4.18 (s, 4H, NCH₂), 3.75 (s, 6H, OMe), 2.52 (t, *J* = 2.4 Hz, 1H, CH). ¹³C-NMR (75 MHz, CDCl₃): δ 171.83 (CO esters), 149.38 (C Ar), 139.73 (C Ar), 122.55 (CH Ar), 122.42 (CH Ar), 119.56 (CH Ar), 115.37 (CH Ar), 78.80 (C≡CH), 75.37 (C=C₂H), 56.81 (OCH₂), 53.77 (NCH₂), 51.82 (OMe). MS (ES⁺), calcd for C₁₅H₁₇NO₅Na [M + Na]⁺ 314.1, found 314.4. HRMS (ES⁺), calcd for C₁₅H₁₈NO₅ [M + H]⁺ 292.1179, found 292.1197.

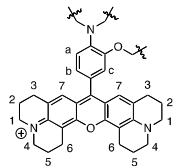
5. To a solution of **4** (3.06 g, 10.51 mmol) in DMF (10 mL) was slowly added POCl₃ (7.82 mL, 84.08 mmol, 8 eq). The mixture turned black and was allowed to stir at 80°C for 3 hours before being cooled down to room temperature. The mixture was then poured in water (1L) and the product was extracted with EtOAc (3 times) and washed with brine twice. The organic phase was dried over MgSO₄, filtered and evaporated to 50 mL EtOAc. The product precipitated under cooling and was filtered to obtain 2.262 g of **5** (67%) as a beige powder. ¹H-NMR (300 MHz, CDCl₃): δ 9.83 (s, 1H, CHO), 7.48-7.43 (m, 2H, H Ar), 6.80 (d, *J* = 8.2 Hz, 1H, H Ar), 4.74 (d, *J* = 2.2 Hz, 2H, OCH₂), 4.25 (s, 4H, NCH₂), 3.81 (s, 6H, OMe), 2.56 (t, *J* = 2.1 Hz, 1H, CH). ¹³C-NMR (75 MHz, CDCl₃): δ 190.45 (CHO), 171.18 (CO esters), 148.33 (C Ar), 145.36 (C Ar), 129.95 (C Ar), 127.12 (CH Ar), 116.91 (CH Ar), 112.81 (CH Ar), 77.72 (C≡CH), 76.10 (C=C₂H), 56.71 (OCH₂), 54.08 (NCH₂), 52.16 (OMe). MS (CI), calcd for C₁₆H₁₈NO₆ [M+H]⁺ 320.1, found 320.1, HRMS (CI), C₁₆H₁₈NO₆ [M+H]⁺ 320.1129, found 320.1191.

8. To a solution of **5** (500 mg, 1.567 mmol) and methyl 2-azido acetate (360 mg, 3.134 mmol, 2 eq) in dioxane (16 mL) was added an heterogeneous solution of CuSO₄·5H₂O (195 mg, 0.783 mmol, 0.5 eq) and sodium ascorbate (217 mg, 1.097 mmol, 0.7 eq) in water (1 mL). The mixture was stirred at 50°C overnight before being extracted with DCM and washed successively with water and brine. The organic phase was dried over MgSO₄, evaporated and the crude was purified by column chromatography on silica gel (EtOAc) to obtain 571 mg of **8** (83%) as a yellowish syrup. Rf=0.40 (100% EtOAc). ¹H-NMR (300 MHz, CDCl₃): δ 9.72 (s, 1H, CHO), 7.75 (s, 1H, H triazol), 7.42 (d, *J* = 1.8 Hz, 1H, H Ar), 7.33 (dd, *J* = 8.2, 1.8 Hz, 1H, H Ar), 6.71 (d, *J* = 8.2 Hz, 1H, H Ar), 5.18 (s, 2H, CH₂COOMe), 5.12 (s, 2H, OCH₂), 4.12 (s, 4H, NCH₂), 3.74 (s, 3H, OMe), 3.60 (s, 6H, OMe). ¹³C-NMR (75 MHz, CDCl₃): δ 190.52 (CHO), 171.15 (CO esters), 166.53 (COOMe), 149.08 (C Ar), 145.37 (C Ar), 143.31 (C Ar), 130.11 (CH Ar), 126.62 (CH triazol), 124.92 (CH Ar), 117.04 (CH Ar), 112.79 (CH Ar), 62.52 (CH₂COOMe), 53.90 (NCH₂), 53.13 (OMe), 52.00 (2 OMe), 50.77 (OCH₂). MS (CI), calcd for C₁₉H₂₃N₄O₈ [M + H]⁺ 435.1, found 435.0. HRMS (ES⁺), calcd for C₁₉H₂₃N₄O₈ [M + H]⁺ 435.1510, found 435.1516.

11. To a solution of **5** (409 mg, 1.282 mmol) and methyl 2-azido acetate (294 mg, 2.564 mmol, 2 eq) in dioxane (15 mL) was added Cp*RuCl(PPh₃)₂ (40 mg, 0.05 mmol, 0.04 eq). The solution was allowed to stir at 90°C. The solutions turned quickly black and a monitoring of the reaction by TLC revealed that the starting material was consumed. The solvent was then evaporated and the crude was purified by column chromatography on silica gel (Cyclohexane/EtOAc : 4/6) to obtain 582mg of **11** (90%) as a yellowish syrup. Rf=0.16 (Cyclohexane/EtOAc : 5/5). ¹H-NMR (300 MHz, CDCl₃): δ 9.83 (s, 1H, CHO), 7.82 (s, 1H, H triazol), 7.48-7.46 (m, 2H, H Ar), 6.84 (d, *J* = 8.6 Hz, 1H, H Ar), 5.34 (s, 2H, OCH₂), 5.19 (s, 2H, CH₂COOMe), 4.12 (s, 4H, NCH₂), 3.79 (s, 3H, OMe), 3.60 (s, 6H, 2 OMe). ¹³C-NMR (75 MHz, CDCl₃): δ 190.25 (CHO), 170.94 (CO esters), 166.96 (CO ester), 148.78 (C Ar), 145.54 (C Ar), 134.82 (CH triazol), 132.47 (C Ar), 130.27 (C Ar), 127.69 (CH Ar), 117.43 (CH Ar), 112.24 (CH Ar), 59.57 (CH₂COOMe), 53.65 (NCH₂), 53.08 (OMe), 52.05 (2 OMe), 49.62 (OCH₂). MS (CI), calcd for C₁₉H₂₃N₄O₈ [M + H]⁺ 435.1, found 435.2. HRMS (ES⁺), calcd for C₁₉H₂₃N₄O₈ [M + H]⁺ 435.1510, found 435.1526.

4.3 Synthesis of X-Rhodamine : typical procedure

Numerotation of X-rhodamines:



6. To a solution of aldehyde **5** (200 mg, 0.626 mmol) in propionic acid was added 8-hydroxyjulolidine (237 mg, 1.254 mmol, 2 eq) and PTSA (11 mg, 0.062 mmol, 0.1 eq). The solution was protected from light and stirred at room temperature overnight. To the brown mixture was added a solution of chloranil (152 mg, 0.626 mmol, 1 eq) in DCM (10 mL), the reaction turned dark and was allowed to stir overnight at room temperature. The dark purple solution was concentrated to dryness, the residue was dissolved in DCM and purified by column chromatography on silica gel (gradient of 100% DCM to 9/1 DCM/Methanol) to obtain 58 mg of **6** (~13%) as a purple solid after lyophilisation (dioxane/water : 1/1). ¹H-NMR (300 MHz, CDCl₃): δ 7.83 (d, *J* = 8.1 Hz, 2H, CH Ar PTSA counter ion), 7.05 (d, *J* = 8.0 Hz, 2H, CH Ar PTSA counter ion), 6.93 (t, *J* = 7.6 Hz, 5H, H_a, H_b, H_c, H₃), 4.70 (d, *J* = 2.2 Hz, 2H, CH₂O), 4.27 (s, 4H, NCH₂), 3.83 (s, 6H, 2 OMe), 3.55 (m, 8H, H₁, H₄), 3.02 (t, *J* = 6.1 Hz, 4H, H₆), 2.73 (t, *J* = 6.0 Hz, 4H, H₃), 2.57 (t, *J* = 2.1 Hz, 1H, C≡CH), 2.27 (s, 3H, Me PTSA counter ion), 2.12-1.98 (m, 8H, H₅, H₂). ¹³C-NMR (75 MHz, CDCl₃): δ 171.73 (CO esters), 154.11 (C Ar), 152.22 (C Ar), 151.04 (C Ar), 148.20 (C Ar), 144.65 (C Ar), 141.08 (C Ar), 138.14 (C Ar), 128.15 (CH PTSA), 126.77 (C₇), 126.29 (CH PTSA), 125.35, 124.10 (CH Ar), 123.56, 118.09 (CH Ar), 116.10 (CH Ar), 112.75, 105.43, 78.00 (C≡CH), 76.28 (C≡CH), 56.78 (CH₂O), 53.87 (NCH₂), 52.15 (2 OMe), 50.95 (C₁ or C₄), 50.48 (C₁ or C₄), 27.73 (C₃), 21.29 (Me PTSA), 20.73 (C₂), 19.96 (C₆), 19.77 (C₅). MS (ES⁺), calcd for C₄₀H₄₂N₃O₆ [M]⁺ 660.3, found 660.7. HRMS (ES⁺), calcd for C₄₀H₄₂N₃O₆ [M]⁺ 660.3068, found 660.3079.

9 was obtained as a purple solid after lyophilisation with ~20% yield. ¹H-NMR (300 MHz, CDCl₃): δ 8.11 (s, 1H, H triazol), 7.71 (d, *J* = 8.1 Hz, 2H, 2CH PTSA), 6.95 (dd, *J* = 4.8, 3.0 Hz, 3H, CH PTSA, 1CH Ar), 6.86-6.73 (m, 4H, CH Ar), 5.22 (s, 2H, CH₂COOMe), 5.11 (s, 2H, OCH₂), 4.16 (s, 4H, NCH₂), 3.68 (s, 3H, OMe), 3.65 (s, 6H, 2 OMe), 3.44 (m, 8H, H₁, H₄), 2.94 (t, *J* = 6.1 Hz, 4H, H₆), 2.69-2.64 (m, 4H, H₃), 2.18 (s, 3H, Me PTSA), 2.02 (t, *J* = 5.1 Hz, 4H, H₅), 1.93-1.91 (m, 4H, H₂). ¹³C-NMR (75 MHz, CDCl₃): δ 171.82 (CO esters), 166.99 (CO ester), 154.70 (C Ar), 152.26 (C Ar), 151.02 (C Ar), 149.12 (C Ar), 144.59 (C Ar), 142.88 (C Ar), 141.13 (C Ar), 138.21 (C Ar), 128.18 (CH PTSA), 127.03 (C₇), 126.23 (CH PTSA), 126.09 (CH triazol), 125.36 (C Ar), 123.63 (C Ar), 123.48 (CH Ar), 117.91 (CH Ar), 115.93 (CH Ar), 112.88 (C Ar), 105.24 (C Ar), 62.56 (OCH₂), 53.82 (NCH₂), 52.92 (OMe), 52.03 (2 OMe), 50.96 (C₁ or C₄), 50.79 (CH₂COOMe), 50.44 (C₁ or C₄), 27.64 (C₃), 21.28 (Me PTSA), 20.74 (C₂), 19.97 (C₆), 19.81 (C₅). MS (ES⁺), calcd for C₄₃H₄₇N₆O₈ [M]⁺ 775.3, found 776.0. HRMS (ES⁺), calcd for C₄₃H₄₇N₆O₈ [M]⁺ 775.3450, found 775.3473.

12 was obtained as a purple solid after lyophilisation with ~16% yield. ¹H-NMR (300 MHz, CDCl₃): δ 7.73 (d, *J* = 7.9 Hz, 2H, CH PTSA), 7.71 (H triazol) 7.02-6.83 (m, 7H, 2CH PTSA, H_a, H_b, H_c, 2H₇), 5.45 (s, 2H, CH₂COOMe), 5.33 (s, 2H, OCH₂), 4.21 (s, 4H, NCH₂), 3.72 (s, 3H, OMe), 3.70 (s, 6H, 2 OMe), 3.57-3.51 (m, 8H, H₁, H₄), 3.02 (t, *J* = 6.1 Hz, 4H, H₆), 2.77-2.71 (m, 4H, H₃), 2.26 (s, 3H, Me PTSA), 2.13-2.08 (m, 4H, H₅), 2.02-2.00 (m, 4H, H₂). ¹³C-NMR (75 MHz, CDCl₃): δ 171.55 (CO esters), 167.27 (CO ester), 154.00 (C Ar), 152.21 (C Ar), 151.07 (C Ar), 148.62 (C Ar), 144.52 (C Ar), 141.05 (C Ar), 138.23 (C Ar), 134.55 (CH triazol), 133.20 (C Ar), 128.16 (CH PTSA), 126.73 (C₇), 126.16 (CH PTSA), 126.05 (C Ar), 124.12 (CH Ar), 123.77 (C Ar), 118.76 (CH Ar), 116.13 (CH Ar), 112.84 (C Ar), 105.30 (C Ar), 59.91 (OCH₂), 53.51 (NCH₂), 52.94 (OMe), 52.04 (2 OMe), 50.99 (C₁ or C₄), 50.47 (C₁ or C₄), 49.72 (CH₂COOMe), 27.64 (C₃), 21.29 (Me PTSA), 20.71 (C₂), 19.96 (C₆), 19.79 (C₂). MS (ES⁺), calcd for C₄₃H₄₇N₆O₈ [M]⁺ 775.3450, found 775.7. HRMS (ES⁺), calcd for C₄₃H₄₇N₆O₈ [M]⁺ 775.3450, found 775.3495.

4.4 Saponification : typical procedure

13. To a solution of **12** (90 mg, ~0.10 mmol) in methanol (10 mL) were added 700 mg of KOH and water (3 mL), the mixture was stirred overnight. The product was washed with aq HCl (1M) and extracted with CHCl₃ until the aqueous phase become slightly pink. The organic phase was then dried over MgSO₄, filtered and concentrated. The residue was purified on a reverse phase column C-18 using acetonitrile (0.1% TFA) and water (0.1% TFA) as eluant (20% ACN to 60%), monitored at 254 nm. The solvents were evaporated and 64 mg of **13** (76%) were obtained as a purple solid after lyophilisation (dioxane/water, 1/1). HRMS (ES⁺), calcd for C₄₀H₄₁N₆O₈ [M]⁺ 733.2980, found 733.3002.

7 was obtained as a purple solid after lyophilisation with ~74% yield. HRMS (ES⁺), calcd for C₃₈H₃₈N₃O₆ [M]⁺ 632.2755, found 632.2761.

10 was obtained as a purple solid after lyophilisation with ~81% yield. HRMS (ES⁺), calcd for C₄₀H₄₁N₆O₈ [M]⁺ 733.2980, found 733.3002

4.5 Dextran Conjugates

Dextran 6,000 MW (Sigma-Aldrich, ref: 31388) and dextran 1,500 MW (Sigma-Aldrich, ref: 31394) were functionalised with **14**²⁹ (see SI) using a method described by Nielsen *et al.*³⁰ The ¹H-NMR showed that the functionalised dextrans were alkylated once per glucose unit.

Journal Name

Final MW Dextran 6,000 : ~14,500 g.mol⁻¹Final MW Dextran 1,500 : ~3,600 g.mol⁻¹

Conjugation of Dextrans. To a solution of dextran-PEG-N₃ (1,500 or 6,000) (40 mg, ~100 μmol glucose unit) and **7** (10 mg, 14 μmol) in DMF (2 mL) was added an heterogeneous solution of CuSO₄·5H₂O (10 mg, 40 μmol) and sodium ascorbate (10 mg, 50 μmol) in water (1 mL). The solution was allowed to stir in the dark at 50°C overnight. The solvents were evaporated, the crude was dissolved in 1 mL of EDTA solution (0.1 M) and passed through a G-25 column to give 40 mg of CaRu-Dextran 6,000 conjugate (~80% yield) and 38 mg CaRu-Dextran 1,500 conjugate (~76% yield).

Acknowledgements

This work was supported by the French Agence National de la Recherche (ANR P3N, nanoFRET2 grant, to J.M.M.)

Notes and references

^a Laboratoire de Biophotonique et Pharmacologie, UMR 7213 CNRS, Université de Strasbourg, Faculté de Pharmacie, 74, Route du Rhin, 67401 Illkirch, France. E-mail: mayeul.collot@unistra.fr

^b Wolfson Institute for Biomedical Research and Department of Neuroscience, Physiology and Pharmacology, University College London, Gower Street, London WC1E 6BT, UK

^c Laboratory of Biomolecules (LBM), UPMC Université Paris 06, Paris F-75005, France

^d Ecole Normale Supérieure (ENS), Paris F-75005, France

^e CNRS, UMR 7203, Paris F-75005, France

Supplementary Information

Experimental data: details of the organic synthesis of probes (HPLC, NMR, mass spectra) and measurements of their photophysical properties are available.

¹ Paredes, R. M.; Etzler, J. C.; Watts, L. T.; Zheng, W.; Lechleiter, J. D. *Methods* 2008, **46**, 143.

² Palmer, A. E. *ACS Chem. Biol.* 2009, **4**, 157.

³ G. Gryniewicz, M. Poenie, R.Y. Tsien, *J. Biol. Chem.* 1985, **260**, 3440.

⁴ Kao, J. P.; Harootunian, A. T.; Tsien, R. Y. *J. Biol. Chem.* 1989, **264**, 8179.

⁵ Thomas, D.; Tovey, S. C.; Collins, T. J.; Bootman, M. D.; Berridge, M. J.; Lipp, P. *Cell Calcium* 2000, **28**, 213.

⁶ Bannwarth, M.; Corrêa, I. R.; Sztretye, M.; Pouvreau, S.; Feally, C.; Aebischer, A.; Royer, L.; Rios, E.; Johnsson, K. *ACS Chem. Biol.* 2009, **4**, 179.

⁷ Egawa, T.; Hanaoka, K.; Koide, Y.; Ujita, S.; Takahashi, N.; Ikegaya, Y.; Matsuki, N.; Terai, T.; Ueno, T.; Komatsu, T.; Nagano, T. *J. Am. Chem. Soc.* 2011, **133**, 14157.

⁸ Oheim, M.; van 't Hoff, M.; Feltz, A.; Zamaleeva, A.; Mallet, J.-M.; Collot, M. *Biochim. Biophys. Acta-Mol. Cell Res.* 2014, **843**, 2284.

- ⁹ Collot, M.; Loukou, C.; Yakovlev, A. V.; Wilms, C. D.; Li, D.; Evrard, A.; Zamaleeva, A.; Bourdieu, L.; Leger, J.-F.; Ropert, N.; Eilers, J.; Oheim, M.; Feltz, A.; Mallet, J.-M. *J. Am. Chem. Soc.* 2012, **134**, 14923.
- ¹⁰ Levy, L.A.; Murphy, E.; Raju, B.; London, R.E. *Biochemistry* 1988, **27**, 4041.
- ¹¹ Kim, H. J.; Han, J. H.; Kim, M. K.; Lim, C. S.; Kim, H. M.; Cho, B. R. *Angew. Chem. Int. Ed* 2010, **49**, 6786.
- ¹² (a) Arunkumar, E.; Ajayaghosh, A.; Daub, J. *J. Am. Chem. Soc.* 2005, **127**, 3156–64. (b) Ashokkumar, P.; Ramakrishnan, V. T.; Ramamurthy, P. *Eur. J. Org. Chem.* 2009, **34**, 5941.
- ¹³ Lallana, E.; Riguera, R.; Fernandez-Megia, E. *Angew. Chem. Int. Ed.* 2011, **50**, 8794.
- ¹⁴ Byrne, J. P.; Kitchen, J. A.; Gunnlaugsson, T. *Chem. Soc. Rev.* 2014, **43**, 5302.
- ¹⁵ Juriček, M.; Kouwer, P. H. J.; Rowan, A. E. *Chem. Commun.* 2011, **47**, 8740.
- ¹⁶ Kushwaha, D.; Singh, R. S.; Tiwari, V. K. *Tetrahedron Lett.* 2014, **55**, 4532.
- ¹⁷ Christensen, J. A.; Fletcher, J. T. *Tetrahedron Lett.* 2014, **55**, 4612.
- ¹⁸ Vedamalai, M.; Wu, S.-P. *Eur. J. Org. Chem.* 2012, **6**, 1158.
- ¹⁹ Shi, W.-J.; Liu, J.-Y.; Ng, D. K. P. *Chem. Asian J.* 2012, **7**, 196.
- ²⁰ Boren, B. C.; Narayan, S.; Rasmussen, L. K.; Zhang, L.; Zhao, H.; Lin, Z.; Jia, G.; Fokin, V. V. *J. Am. Chem. Soc.* 2008, **130**, 8923.
- ²¹ Song, F.; Watanabe, S.; Floreancig, P. E.; Koide, K. *J. Am. Chem. Soc.* 2008, **130**, 16460.
- ²² Zhang, S.; Geng, J.; Yang, W.; Zhang, X. *RSC Adv.* 2014, **4**, 12596.
- ²³ Jiang, P.; Guo, Z. *Coordination Chemistry Reviews* 2004, **248**, 205.
- ²⁴ See section « Dextran conjugates » at <http://www.lifetechnologies.com>
- ²⁵ (a) Ansorge, W.; Pepperkok, R. *J. Biochem. Biophys. Methods* 1988, **16**, 283. (b) Pepperkok, R.; Zanetti, M.; King, R.; Delia, D.; Ansorge, W.; Philipson, L.; Schneider, C. *Proc. Natl. Acad. Sci. USA* 1988, **85**, 6748. (c) Fishkind, D. J.; Cao, L. G.; Wang, Y. L. *J Cell Biol* 1991, **114**, 967.
- ²⁶ Collot, M.; Lasoroski, A.; Zamaleeva, A. I.; Feltz, A.; Vuilleumier, R.; Mallet, J.-M. *Tetrahedron* 2013, **69**, 10482.
- ²⁷ Berlin, J.; Konishi, M. *Biophys. J.* 1993, **65**, 1632.
- ²⁸ Buon, C.; Chacun-Lefèvre, L.; Rabot, R.; Bouyssou, P.; Coudert, G. *Tetrahedron* 2000, **56**, 605.
- ²⁹ Knapp, D. C.; D'Onofrio, J.; Engels, J. W. *Bioconjugate chem.* 2010, **21**, 1043.
- ³⁰ Nielsen, T. T.; Wintgens, V.; Amiel, C.; Wimmer, R.; Larsen, K. L. *Biomacromolecules* 2010, **11**, 1710.

